Outskirts of Galaxy Clusters: Intense Life in the Suburbs
Proceedings IAU Colloquium No. 195, 2004
A. Diaferio, ed.

DOI: 10.1017/S1743921304000249

First detection of WHIM filaments at cosmological distances

Fabrizio Nicastro

Harvard-Smithsonian Center for Astrophysics, 60 Garden Street, Cambridge, MA 02138, USA
email: fnicastro@cfa.harvard.edu

Abstract. In this contribution we present the detection of two WHIM filaments in the *Chandra*-LETG spectrum of Mkn 421. This spectrum has been obtained following 2 of our pre-approved Target of Opportunity requests to observe Blazars in outburst to efficiently 'X-ray' the IGM at high spectral resolution. These observations caught the source at the unprecedented levels of 60 and 40 mCrab in the soft X-ray (0.5-2 keV) band. We detect, for the first time, two WHIM filaments at redshifts of z=0.011 and z=0.027, respectively. Based on these two detections and on the upper limits on associated HI and OVI absorption as inferred from the HST and FUSE spectra of Mkn 421, we estimate a number of WHIM filaments per unit redshift, with He-like ion columns $N_X \gtrsim 8 \times 10^{14}$ cm^{-2} of $dN/dz = 67^{+88}_{-43}$, and a baryon mass density of $\Omega_b = 0.021^{+0.028}_{-0.014}$, virtually all of the 'missing baryons' at $z < 1$.

1. Introduction

Despite recent progress in cosmology, very little is still known about the location of baryons in the local Universe. The number of baryons detected in the "virialized Universe" at $z \lesssim 2$ (i.e. stars, neutral hydrogen associated with galaxies, and X-ray emitting gas in clusters) is more than a factor of 2 smaller than the concordance cosmology value of $\Omega_b = (4.4 \pm 0.4) h_{70}^{-2}$ % (Bennett *et al.* 2003), i.e. $\Omega_b < 2 h_{70}^{-2}$ % (2σ; e.g. Fukugita, Hogan & Peebles 1998).

Hydrodynamical simulations for the formation of structures in the Universe, offer a possible solution to this puzzle. They predict that in the present epoch ($z \lesssim 1-2$), half of the normal baryonic matter in the Universe (the "missing baryons") is in a tenuous (overdensities $\delta \simeq 5-50$, relative to the mean baryon density in the Universe) warm-hot ($T = 10^{5.5} - 10^7$ K) phase, the so called 'Warm Hot Intergalactic Medium' (WHIM, e.g. Hellsten *et al.* 1998; Cen & Ostriker, 1999; Davé *et al.* 2001). This filamentary web of gas should imprint a 'forest' of metal absorption lines in the soft X-ray spectra of background sources. However, the vast majority of WHIM filaments is expected to be very thin, with metal ion columns typically much lower than $N_X \sim 10^{16}$ cm^{-2} (e.g. Fang, Bryan & Canizares, 2002).

A Local Group system of WHIM-like gas has been detected in X-ray species (Nicastro *et al.* 2002, Fang, Sembach & Canizares 2003, Rasmussen, Kahn & Paerels 2003, Cagnoni *et al.* 2004) and in high-velocity UV OVI (Nicastro *et al.* 2003). No secure detection of intervening WHIM absorption systems at cosmological distances has been claimed so far. We present the first high significance ($\gtrsim 5.8\sigma$ and $\gtrsim 11\sigma$) detection of two $z > 0$ WHIM filaments, in a high signal-to-noise *Chandra*-LETG spectrum of the blazar Mkn 421.

Throughout the paper we assume $H_0 = 70$ km s^{-1} Mpc^{-1}. Errors are quoted at 1σ for interesting parameters, unless otherwise stated.

2. Detecting the WHIM

With the exception of the very high-density tail of the intergalactic medium mass distribution (i.e. $\delta \gtrsim 1000$), in proximity of the most complex nodes of the WHIM web (i.e. outskirts of clusters of galaxies: Kaastra this conference), the vast majority of WHIM filaments should give rise to line emissions way below the sensitivity threshold of current X-ray instruments (e.g. Yoshikawa et al. 2003). Metal absorption lines from the WHIM, instead, can now in principle be detected in the *Chandra*-LETG or *Newton*-XMM RGS spectra of bright extragalactic sources, but only if the number of counts per resolution element ($\Delta\lambda = 50$ mÅ) in the continuum adjacent the line is larger than about 500. This number should be compared with the average 10-50 counts per resolution element in the archival *Chandra*-LETG spectra of the brightest Seyfert 1s (about 0.5-1 mCrab in the 0.5-2 keV band), collected, on average, with 100 ks exposures. So, either multi-megasecond integrations of the brightest nearby AGNs or transiently brighter sources are needed to detect the WHIM in absorption.

The public *Rossi* XTE All Sky Monitor (ASM) light curves show that several Blazars whose normal 2-10 keV flux states range between 0.1 and 5 mCrab have factor 10-50 outbursts, reaching 2-10 keV fluxes larger than 5-20 mCrab at least once per year. This flares usually last for a relatively short period of time (normally few days), but during these events these objects are, by far, the brightest extragalactic objects in the X-ray sky (with the exceptions of GRB afterglows that, however, typically are brighter than 1 mCrab only for ~ 1 day). We have pursued the less time-consuming of the two possible observational strategies: to detect the WHIM by waiting for one of these Blazars to flare, and then trigger a fast (i.e. less than 1 day from the trigger) Target of Opportunity Observation (TOO) with either the *Chandra* LETG or the *Newton*-XMM RGS.

We triggered our first two TOOs with the *Chandra*-ACIS-LETG and -HRC-LETG on 2002, October, 26-27, and 2003, July 1-2, on the blazar Mkn 421 ($z = 0.03$, De Vaucouleurs *et al.* 1991). These observations caught the source at 60 and 40 mCrab in the 0.5-2 keV band, and allowed us to collect a total of 6000 counts per resolution element at 21.6 Å. This is sufficient to detect He-like and H-like ion columns of $N_X \gtrsim 8 \times 10^{14}$ cm^{-2} at a significance level $\geqslant 3\sigma$.

3. WHIM absorption in the *Chandra*-LETG spectrum of Mkn 421

Figure 1 shows six portions of the LETG spectrum of Mkn 421. Three different ionized absorption systems are clearly identified in the spectrum: $z \sim 0$ (made up of both ISM, i.e. Savage *et al.* 2000, and Local-Group IGM lines, Nicastro *et al.* 2002, 2003), $z = 0.011$ (hereinafter WHIM System-I) and $z = 0.027$ (hereinafter WHIM System-II). The strongest line from WHIM System-I is the OVII$_{K\alpha}$ (N$_{OVII} = (1.0 \pm 0.3) \times 10^{15}$ cm^{-2}), while the two strongest lines of WHIM System-II are NVII$_{K\alpha}$ (N$_{NVII} = (1.5 \pm 0.4) \times 10^{15}$ cm^{-2}) and NVI$_{K\alpha}$ (N$_{NVI} = (0.7 \pm 0.2) \times 10^{15}$ cm^{-2}). We caution that, although clearly seen in the spectrum (Fig. 1), the NeIX$_{K\alpha}$ and OVII$_{K\beta}$ from System-II, as well as the OVIII$_{K\alpha}$ line from the System-I, lie very close to chip-gaps edges, which may induce an over-estimate of their EWs. We therefore consider the EWs of these lines only as upper-limits.

4. WHIM absorption in the UV spectra of Mkn 421

Mkn 421 has been observed with the HST-GHRS on 1995 February 1. An intervening HI Lyα system at $cz = (3046 \pm 2)$ km s^{-1} was discovered and reported by Shull *et al.*

https://doi.org/10.1017/S1743921304000249 Published online by Cambridge University Press

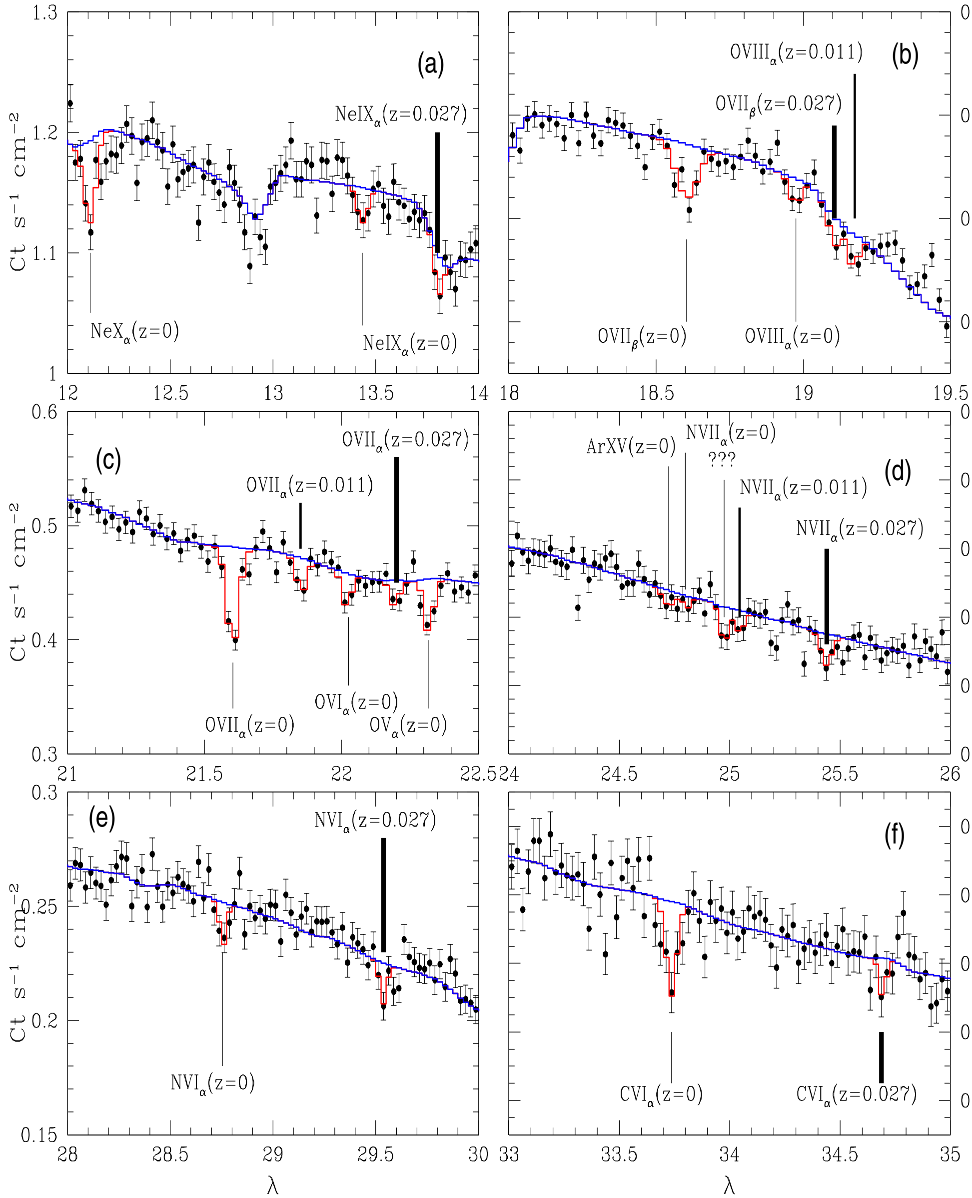

Figure 1. Six portions of the *Chandra*-LETG spectrum of Mkn 421 along with its best fitting continuum plus narrow absorption model (solid line: see details in Nicastro *et al.* 2004, ApJ, submitted), centered around the rest-wavelengths of the (a) NeXI-X$_{K\alpha}$, (b) OVIII$_{K\alpha}$, (c) OVII$_{K\alpha}$, (d) NVII$_{K\alpha}$, (e) NVI$_{K\alpha}$ and (f) CVI$_{K\alpha}$ transitions.

(1996). We retrieved this GHRS spectrum of Mkn 421 from the public HST archive, and re-analyzed the data. We fitted the 1220-1250 Å HST spectrum with a combination of broad continuum components and three narrow absorption Gaussians to model the intervening HI Lyα and two strong Galactic Si lines visible in the spectrum. The redshift of the HI Lyα line (N$_{HI}$ = $(1.65 \pm 0.07) \times 10^{13}$ cm^{-2}) is consistent with that of our

System	T^a	N$_H{}^b$	D^c	[N/O]^d	[O/H]^e	$n_b{}^f$
I ($z = 0.011$)	(0.4-5.7)	(0.9-1.7)	(0.3-0.5)		$\geqslant -0.96$	$\gtrsim 1$
II ($z = 0.027$)	(0.7-1.7)	(1.5-3.0)	(0.5-1)	$\geqslant 0.2$	$\geqslant -0.3$	$>> 0.15$

Table 1. Physical parameters of the WHIM filaments. Units are as follows: ^{a}In 10^6 K. ^{b}In $10^{19}10^{-[O/H]}$ cm^{-2}. ^{c}In $10^{-[O/H]}n_b^{-1}$ Mpc. ^{d}[N/O] = Log$\left(\frac{(N/O)}{(N/O)_\odot}\right)$. ^{e}[H/O] = Log$\left(\frac{(O/H)}{0.1(O/H)_\odot}\right)$. ^{f}In 10^{-5} cm^{-3}.

X-ray WHIM System-I within the large systematic X-ray uncertainties ($\Delta z = 0.001$†). However, the average position of the X-ray system lies at ~ 5 Mpc from the accurate ($\Delta z = 7 \times 10^{-6}$) position of the HI system. Moreover the measured HI Lyα FWHM=0.28 Å gives an upper limit of $T < 2 \times 10^5$ K to the kinetic temperature of the HI, which is inconsistent with the temperature estimated for the X-ray WHIM System-I (see §5). If the systems are related, a multiphase WHIM is required. We also computed the 3σ HI column upper limit of a putative HI Lyα at the average redshift of the X-ray WHIM Systems. For System-I we found N$_{HI} < 3.9 \times 10^{12}$ cm^{-2}. Instead, for System-II we found a line at λ1248.80 Å at a significance of 4.7σ, which we identified with a HI Lyα at $z = 0.0273$ with column of N$_{HI} = (3.3 \pm 0.7) \times 10^{12}$ cm^{-2}. The FWHM of this line is $\leqslant 1.0$ Å, implying $T \lesssim 2 \times 10^6$ K, consistent with the range of estimated HI kinetic temperatures for System-II (see §5).

Mkn 421 was also observed by FUSE on 2003, January 19-21, with a final total exposure time of 62 ks, following our TOO request based on a period of strong X-ray activity as recorded by the RXTE-ASM. We searched the FUSE spectrum of Mkn 421 for OVI$_{2s\rightarrow 2p}$ candidate intervening absorption line in the ~ 1032 to ~ 1062 Å wavelength range (i.e. from $z = 0$ up to to $z = 0.03$, the redshift of the source). With the exception of the strong Galactic Low-Velocity OVI (Savage et al. 2001) and the much weaker and probably extragalactic High Velocity OVI (Williams et al. 2004, in preparation), we did not detect any $z > 0$ OVI absorption down to a 3σ sensitivity limit of N$_{OVI} = 2 \times 10^{13}$ cm^{-2}.

5. Diagnostics analysis of WHIM System-I and -II

To infer the physical properties of the gas in these two WHIM filaments we first applied the equivalent width ratios technique to get direct information on the ionization balance in the gas and its metallicity, and then compared these quantities with predictions by gas ionization models to estimate the temperature and the equivalent H column density of the gas (see e.g. Nicastro et al. 2002, for details). Table 1 lists the physical parameters of the WHIM System-I and -II.

Limits on the baryon density n_b, in Table 1 are derived from the lower limits on [O/H] and from the fact that the total extent D of the filament along our line of sight has to be less than 5 Mpc for System-I (the distance from the average redshift of the X-ray system and that of the cooler HI system) and much lower than 13 Mpc for System-II (the distance of the filament from Mkn 421). We note that, although the ranges of uncertainty are large, physical and geometrical parameters for System-I and -II are all consistent with theoretical predictions for the WHIM. We also note that System-II ($z = 0.027$) tends to

† Errors associated with X-ray line wavelengths are largely dominated by systematics in the LETG wavelength calibrations. We estimated the amplitude of these systematics in our data looking for differences between expected and observed relative positions of two strong lines from the same ion, and then added a 20 mÅ systematic uncertainty to all our X-ray line wavelengths.

be somewhat bigger and more metal rich than System-I ($z = 0.011$), which may reflect a difference in the galaxy-environment in which the two systems lie.

6. dN/dz and Ω_b

Based on these two detections of WHIM filaments, we can now make a first, crude, estimate of the number of filaments per unit redshift with He-like ion columns larger than 8×10^{14} cm^{-2} (our 3σ detection threshold). We obtain $dN/dz(N_X > 8 \times 10^{14}) = 67^{+88}_{-47}$ (1σ, Gehrels 1986), in gratifying agreement with theoretical predictions of $dN/dz(N_X > 8 \times 10^{14}) = 65$.

Similarly, we can estimate the cosmological mass density of X-ray WHIM filaments. Following Savage et al. (2002) we measure $\Omega_b = (\frac{1}{\rho_c})(\frac{\mu m_p \sum_i N_H^i}{d_{Mkn421}}) = 0.021^{+0.028}_{-0.014}$, virtually all the 'missing' baryons at low redshift.

7. Conclusions

We have presented the first detection of two X-ray WHIM filaments at redshifts of $\langle z_1 \rangle = 0.011$ and $\langle z_2 \rangle = 0.027$, in the very high quality *Chandra*-LETG spectrum of the blazar Mkn 421. For System-I we estimate a temperature of $T = (0.4 - 5.7) \times 10^6$ K, an equivalent H column density of $\mathrm{N}_H = (0.9 - 1.7) \times 10^{-[O/H]} \times 10^{19}$ cm^{-2}, a metallicity of [O/H]$\geqslant -0.96$, and a baryon density of $n_b \gtrsim 10^{-5}$ cm^{-3}. For System-II we obtain: $T = (0.7 - 1.7) \times 10^6$ K, $\mathrm{N}_H = (1.5 - 3.0) \times 10^{-[O/H]} \times 10^{19}$ cm^{-2}, [O/H]$\geqslant -0.3$, and $n_b \gg 1.5 \times 10^{-6}$ cm^{-3}. The number of X-ray WHIM filaments per unit redshift and with He-like ion columns larger than 8×10^{14} cm^{-2}, inferred from these two detections is $dN/dz(N_X > 8 \times 10^{14}) = 67^{+88}_{-47}$, in gratifying agreement with theroretical predictions and so sufficient to account for all the 'missing' baryons in the local Universe. The cosmological mass density of X-ray WHIM filaments that we measure is $\Omega_b = 0.021^{+0.028}_{-0.014}$.

Acknowledgements

The author acknowledges the *Chandra* grant GO2-3122A.

References

Bennett, C.L., *et al.* 2003 *ApJS* **148**, 1-27.
Cagnoni, I. *et al.*, 2004 *ApJ* **603**, 449-455.
Cen, R. & Ostriker, J.P., 1999 *ApJ* **514**, 1-6.
Davé, R., *et al.*, 2001 *ApJ* **522**, 473-483.
De Vaucouleurs, G. *et al.*, 1991 *Springer-Verlag Berlin Heidelberg New York* **1-3, XII**, 1-2069.
Fang, T., Bryan, G.L. & Canizares, C.R., 2002 *ApJ* **564**, 604-623.
Fang, T., Sembach, K.R. & Canizares, C.R., 2003 *ApJ* **586**, L49-L52.
Fukugita, M., Hogan, C.J. & Peebles, P.J.E., 1998 *ApJ* **503**, 518-530.
Gehrels, N., 1986 *ApJ* **303**, 336-346.
Hellsten, U., Gnedin, N.Y. & Miralda-Escudé, J., 1998 *ApJ* **509**, 56-61.
Nicastro, F., *et al.*, 2003 *Nature* **421**, 719-721.
Nicastro, F., *et al.*, 2002 *ApJ* **573**, 157-167.
Rasmussen, *et al.* 2003 *ASSL Conference Proceedings* **281**, 109.
Savage, B.D., *et al.* 2002 *ApJ* **564**, 631-649.
Savage, B.D., *et al.* 2000 *ApJ* **538**, L27-L30.
Shull, J.M, Stocke, J.T. & Penton, S., 1996 *AJ* **111**, 72-77.
Yoshikawa, K., *et al.*, 2003 *PASJ* **55**, 879-890.